



HAL
open science

Nonlinear parabolic equation model for finite-amplitude sound propagation over porous ground layers

T. Leissing, P. Jean, J. Defrance, Christian Soize

► **To cite this version:**

T. Leissing, P. Jean, J. Defrance, Christian Soize. Nonlinear parabolic equation model for finite-amplitude sound propagation over porous ground layers. 13th Long Range Sound Propagation Symposium (LRSPS), Ecole Centrale de Lyon, Oct 2008, Ecully, France. pp.1-11. hal-00691732

HAL Id: hal-00691732

<https://hal.science/hal-00691732>

Submitted on 26 Apr 2012

HAL is a multi-disciplinary open access archive for the deposit and dissemination of scientific research documents, whether they are published or not. The documents may come from teaching and research institutions in France or abroad, or from public or private research centers.

L'archive ouverte pluridisciplinaire **HAL**, est destinée au dépôt et à la diffusion de documents scientifiques de niveau recherche, publiés ou non, émanant des établissements d'enseignement et de recherche français ou étrangers, des laboratoires publics ou privés.

Nonlinear parabolic equation model for finite-amplitude sound propagation over porous ground layers

T. Leissing^{a,*}, P. Jean^a, J. Defrance^a and C. Soize^b

^a*CSTB, 24 rue Joseph Fourier, 38400 Saint Martin d'Hères, France*

^b*Université Paris-Est, Laboratoire Modélisation et Simulation Multi Echelle, MSME FRE3160 CNRS, 5 bd Descartes, 77454 Marne-la-Vallée, France*

Abstract

The nonlinear parabolic equation (NPE) is a time-domain method widely used in underwater sound propagation applications. It allows simulating weakly nonlinear sound propagation within an inhomogeneous medium. For this method to be suited for outdoor applications, it must account for the effects of an absorbing ground surface. The NPE being formulated in the time domain, complex impedances cannot be used. The ground layer is thus included in the computational system with the help of a second NPE model based on the Zwikker-Kosten model. A two-way coupling between these two layers (air and ground) is required for the whole system to behave correctly. Coupling equations are derived from linearized Euler equations. In the frame of a (small-angle) parabolic model, this two-way coupling only involves spatial derivatives, making its implementation easy. Several propagation examples are then presented, and the method is shown to give satisfactory results for a wide range of ground characteristics. Finally, the problem of including Forchheimer's nonlinearities in the two-way coupling is addressed and an approximate solution is proposed.

Key words: nonlinear propagation, NPE, parabolic equation, porous ground, Forchheimer's nonlinearities

1. Introduction

Due to their high amplitudes, sound waves from explosions propagate over large distances. The need to develop numerical models that can handle main features of finite-amplitude sound propagation outdoors is obvious. Specifically, in addition to nonlinearities, numerical models must take into account meteorological and ground effects (refraction, dissipation, hilly terrain, ground impedance).

In this work a nonlinear parabolic equation (NPE) model is used to simulate finite amplitude sound propagation. This method has first been developed by McDonald and Kuperman in 1987 [1] and has been successfully used for underwater acoustics simulations [2,3]. It has also been used together with other methods to simulate blast wave propagation in air [4-7]. In this article, the method is adapted to handle sound propagation over impedant ground surfaces.

The fundamental principle of the NPE is the resolution of a simplified nonlinear wave equation over a moving window surrounding the wavefront. This implies that the method is suitable for finite-length

* Corresponding author.

Email address: thomas.leissing@cstb.fr (T. Leissing).

signals only. As the calculation domain is limited to a small area around the signal, computational cost is greatly reduced compared to Euler's equations methods. On the other hand backward propagation cannot be accounted for. For the derivation of the NPE model, the reader may refer to articles by McDonald[8] or Caine and West[9]. The simplest formulation of the NPE is[1,10]:

$$D_t R = -\partial_x \left(c_1 R + c_0 \frac{\beta}{2} R^2 \right) - \frac{c_0}{2} \int \nabla_{\perp}^2 R dr \quad (1)$$

where t is the time variable, x is the main propagation direction, ∇_{\perp}^2 is the transverse Laplacian, c_0 is the ambient sound speed, c_1 is the sound speed perturbation in the window and $R = \rho' / \rho_0$, with ρ the acoustic density perturbation and ρ_0 the ambient medium density. For air, the coefficient of nonlinearity β is calculated with the help of the ratio of specific heat at constant volume and pressure γ , *i.e.* $\beta = (\gamma + 1) / 2$, and is approximately equal to 1.2 for air under normal conditions. The sound speed $c(x, y)$ is allowed to vary within the domain. The first term on the right hand side of Eq (1) simulates refraction and nonlinear effects; the second term calculates diffraction. The transverse Laplacian operator reduces to ∂_z^2 for a 2D Cartesian domain, where z is the transverse propagation direction. D_t is a moving window operator and is defined by:

$$D_t = \partial_t + c_{win} \partial_x \quad (2)$$

where c_{win} is the moving window celerity. Eq (1) can be used to propagate weak shocks over moderate distance within a domain with spatially-varying sound speed. Various modifications and additions to this original model were made during the past two decades : spherical and cylindrical formulations [11], thermoviscous effects [12], high-angle formulation [13], propagation in multiple medium [2], propagation through turbulence [14]...

In this work, a NPE model that includes the effects of a soft ground on propagation is proposed. The ground layer, characterized by a Zwikker–Kosten (ZK) model, is included as a propagation medium in the calculations. The derivation of the NPE model for porous ground layers is described in section 2. Combined with a boundary interface condition, presented in section 3, and a NPE model for atmospheric media, it allows to simulate finite-amplitude sound propagation over an impedant ground surface. Several propagation examples are then presented and finally, an approximate solution to include Forchheimer's nonlinearities in the two-way coupling is presented.

2. NPE model for rigidly-framed porous media

The domain considered is two-dimensional with main axes x (horizontal direction) and z (vertical direction). Total density ρ_T and total pressure p_T variables are noted as follows:

$$\rho_T = \rho_0 + \rho' \quad (3a)$$

$$p_T = p_0 + p' \quad (3b)$$

where ρ_0 and p_0 are ambient density and ambient pressure, respectively, and ρ' and p' are acoustic perturbations of these quantities. Components of the flow velocity vector \mathbf{V} are u and w , which are the flow velocities in the x - and z -directions, respectively. Partial derivation with respect to the variable i is noted ∂_i .

The nonlinear parabolic equation (NPE) model for sound propagation in porous ground media is based on a nonlinear extension of the Zwikker–Kosten (ZK) model [15]. The ground is considered equivalent to a continuous fluid for sound waves. A sound wave causes a vibration of air particles contained in the ground pores, while the ground frame does not vibrate. The ground layer is characterized by a set of 4 parameters: the DC flow resistivity σ_0 , the porosity Ω_0 , the tortuosity Φ and the Forchheimer's nonlinearity parameter ξ . These quantities are assumed fixed in space and time. In this context, equations of continuity and conservation of momentum are [16–18]:

$$\partial_t \rho_T + \partial_x (\rho_T u) + \partial_z (\rho_T w) = 0 \quad (4a)$$

$$\Phi \partial_t (\rho_T u) + \partial_x (p_T + \Phi \rho_T u^2) + \partial_z (\Phi \rho_T u w) + \sigma_0 \Omega_0 (1 + \xi |u|) u = 0 \quad (4b)$$

$$\Phi \partial_t (\rho_T w) + \partial_z (p_T + \Phi \rho_T w^2) + \partial_x (\Phi \rho_T u w) + \sigma_0 \Omega_0 (1 + \xi |w|) w = 0 \quad (4c)$$

Combining Eqs (4) and eliminating terms of third order in x -derivatives and of second order in z -derivatives gives:

$$\Phi \partial_t^2 \rho_T = \partial_x^2 (p_T + \Phi \rho_0 u^2) + \partial_z^2 p_T + \sigma_0 \Omega_0 \partial_x [(1 + \xi |u|) u] + \sigma_0 \Omega_0 \partial_z w \quad (5)$$

To find an expression for the flow velocities u and w we use the perturbation expansions method. The same scalings and expansions as in refs [1,8] are used (however, note that the sound speed in the ground layer is $c_0/\sqrt{\Phi}$). Eq (4a) can be rewritten:

$$\left(\epsilon \partial_t - \frac{c_0}{\sqrt{\Phi}} \partial_x \right) (\rho_0 + \epsilon \rho'_1 + \epsilon^2 \rho'_2 + \dots) = - \partial_x \left[(\rho_0 + \epsilon \rho_1 + \epsilon^2 \rho_2 + \dots) (\epsilon u_1 + \epsilon^{3/2} u_2 + \dots) \right] - \epsilon^{1/2} \partial_z \left[(\rho_0 + \epsilon \rho_1 + \epsilon^2 \rho_2 + \dots) (\epsilon w_1 + \epsilon^{3/2} w_2 + \dots) \right] \quad (6)$$

Equating terms of order ϵ and $\epsilon^{3/2}$ gives:

$$u_1 = \frac{c_0}{\sqrt{\Phi}} \frac{\rho_1}{\rho_0} \quad (7a)$$

$$w_1 = 0 \quad (7b)$$

Note that $\rho' = \rho_1 + O(\epsilon^2)$, $u = u_1 + O(\epsilon^{3/2})$ and $w = w_1 + O(\epsilon^{3/2})$. Substitution of u and w by u_1 and w_1 in Eq (5) leads to an error consistent with the accuracy sought. The total pressure p_T is substituted by a second-order expansion in ρ' from an assumed adiabatic equation of state:

$$p_T = p_0 + c_0^2 \rho' + c_0^2 \left(\frac{\gamma - 1}{2\rho_0} \right) \rho'^2 \quad (8)$$

where γ is the ratio of specific heats at constant pressure and volume. Inserting Eq (8) in Eq (5) yields:

$$\Phi \partial_t^2 \rho' = c_0^2 \partial_x^2 \left[\rho' + \left(\frac{\gamma + 1}{2\rho_0} \right) \rho'^2 \right] + c_0^2 \partial_z^2 \rho' + \frac{\sigma_0 \Omega_0 c_0}{\rho_0 \sqrt{\Phi}} \partial_x \left[\left(1 + \frac{\xi c_0}{\sqrt{\Phi}} \left| \frac{\rho'}{\rho_0} \right| \right) \rho' \right] \quad (9)$$

A “moving-frame” operator D_t^* is introduced:

$$D_t^* = \partial_t + \frac{c_0}{\sqrt{\Phi}} \partial_x \quad (10)$$

The parabolic approximation gives [9]:

$$\partial_t^2 \longrightarrow -2 \frac{c_0}{\sqrt{\Phi}} D_t^* \partial_x + \frac{c_0^2}{\Phi} \partial_x^2 \quad (11)$$

Replacing the second time derivative in Eq (9) and rearranging gives a NPE model for propagation in porous media:

$$D_t^* R = - \frac{c_0}{\sqrt{\Phi}} \partial_x \left(\frac{\beta}{2} R^2 \right) - \frac{c_0}{2\sqrt{\Phi}} \int \partial_z^2 R dx - \frac{\sigma \Omega}{2\Phi \rho_0} \left(1 + \frac{\xi c_0}{\sqrt{\Phi}} |R| \right) R \quad (12)$$

where β is the hydrodynamic nonlinearity parameter and R is a dimensionless density perturbation ($R = \rho'/\rho_0$). Eq (12) can be used to simulate sound propagation within a porous ground layer. However, if one wants to couple air/ground models, a last modification must be done. Indeed, both models use different frame speeds: c_0 and $c_0/\sqrt{\Phi}$. Correcting for the frame-speed difference leads to the following substitution:

$$D_t^* \longrightarrow D_t + \frac{c_0}{\sqrt{\Phi}} (1 - \sqrt{\Phi}) \partial_x \quad (13)$$

Eq (12) becomes:

$$D_t R = - \frac{c_0}{\sqrt{\Phi}} \partial_x \left[(1 - \sqrt{\Phi}) R + \frac{\beta}{2} R^2 \right] - \frac{c_0}{2\sqrt{\Phi}} \int \partial_z^2 R dx - \frac{\sigma \Omega}{2\Phi \rho_0} \left(1 + \frac{\xi c_0}{\sqrt{\Phi}} |R| \right) R \quad (14)$$

The NPE model described by Eq (14) is able to simulate finite amplitude sound propagation *within* a rigid, framed, porous material described by a set of 3+1 parameters. Note that if $\Phi = 1$ and losses in the layer are neglected, the model exactly reduces to the usual NPE model for atmospheric propagation (Eq (1), [19]). Eq (14) allows to draw some conclusions about finite-amplitude sound propagation in porous media: (a) the sound speed in the medium is inversely proportional to the square root of the material tortuosity, *i.e.* $c = c_0/\sqrt{\Phi}$; (b) the attenuation in the ground layer is composed of a linear term (the term containing $\sigma_0\Omega_0$ term) plus a nonlinear term (the term containing ξ); (c) in the frame of this model, the material resistivity is proportional to the overdensity R .

3. Derivation of a boundary interface condition

3.1. Derivation

As both models use the same moving-frame speed, they can be combined to simulate finite-amplitude sound propagation over a rigidly-framed porous ground layer. This section aims at establishing a first-order boundary interface condition to couple these two propagation models. The variables $p'_{i,j}{}^a$ and $p'_{i,j}{}^g$ are introduced to denote quantities in layer A (air layer) and layer G (porous ground layer), respectively, at range $i\Delta x$ in the moving window and altitude $j\Delta z$. The fluid-fluid interface is taken to be midway between two vertical grid points with indexes $j = 0$ and $j = 1$. Auxiliary virtual points $p'_{i,0}{}^a$ and $p'_{i,1}{}^b$ are created (see Figure 1). In the following we assume that the deformation of the interface by the wave is small [2].

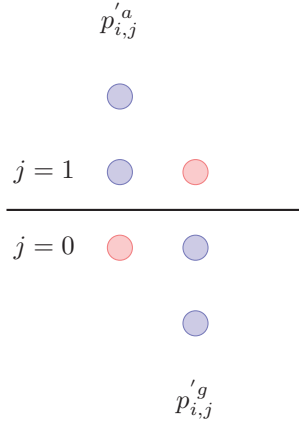


Fig. 1. The fluid-fluid interface is taken to be midway between two vertical grid points with indexes $j = 0$ and $j = 1$. Auxiliary virtual points (red circles) $p'_{i,0}{}^a$ and $p'_{i,1}{}^g$ are created.

Interfacial boundary conditions are continuity of pressure and normal flow velocity:

$$[p'^a] = [p'^g] \quad [w^a] = [w^g] \quad (15)$$

where the square brackets denote a quantity across the interface. We seek for expressions of w^a and w^g involving the pressure disturbance p' to the first order. As a first order boundary interface condition is sought, linearized equations are used; for the air layer A we use the linearized Euler equation:

$$\rho_0 \partial_t (w^a) = -\partial_z p_T^a \quad (16)$$

The perturbation expansion method is used and the same scalings as in section 2 and in refs [1,8] are used. Rewriting Eq (16) and equating terms of order 1 and 3/2 gives:

$$w_1^a = 0 \quad w_2^a = (\rho_0 c_w \partial_x)^{-1} \partial_z p_1^a \quad (17)$$

Note that $w^a = w_1^a + w_2^a + O(\epsilon^{5/2})$. To the order of accuracy sought in this work it can be written:

$$w^a = (\rho_0 c_0 \partial_x)^{-1} \partial_z p_1^a \quad (18)$$

To find an expression for w^g we start from the following equation [20]:

$$\Phi\rho_0\partial_t w^g = -\Omega_0\partial_z p_T^g - \sigma_0\Omega_0 w^g \quad (19)$$

The same procedure is applied; one can find:

$$w^g = \left(\sqrt{\Phi}\rho_0 c_0 \partial_x - \sigma_0 \Omega_0\right)^{-1} \Omega_0 \partial_z p_1^g \quad (20)$$

The interfacial condition for the continuity of vertical velocities w^a and w^g can now be written:

$$\left[(\rho_0 c_0 \partial_x)^{-1} \partial_z p^a\right] = \left[\left(\sqrt{\Phi}\rho_0 c_0 \partial_x - \sigma_0 \Omega_0\right)^{-1} \Omega_0 \partial_z p^g\right] \quad (21)$$

Rearranging Eq (21) leads to:

$$\left[\sqrt{\Phi}\partial_z p^a - \frac{\sigma_0 \Omega_0}{\rho_0 c_0} \int \partial_z p^a dx\right] = \left[\Omega_0 \partial_z p^g\right] \quad (22)$$

A trapezoidal law and finite-differences expressions for p^a and p^g and their derivatives are used to discretize Eq (22). For a layer l we use:

$$\left[p^l\right] = \frac{p_{i,1}^l + p_{i,0}^l}{2} \quad (23a)$$

$$\left[\partial_z p^l\right] = \left(p_{i,1}^l - p_{i,0}^l\right) \Delta z^{-1} \quad (23b)$$

Replacing these approximations into Eq (22) gives expressions for unknown quantities $p_{i,0}^a$ and $p_{i,1}^g$:

$$p_{i,0}^a = \left(\frac{A_1 - G_1}{A_0 + G_1}\right) p_{i,1}^a + \left(\frac{G_0 + G_1}{A_0 + G_1}\right) p_{i,0}^g + \left(\frac{S_A}{A_0 + G_1}\right) \sum_{m=N_x}^{i+1} \left(p_{m,1}^a - p_{m,0}^a\right) \quad (24a)$$

$$p_{i,1}^g = \left(\frac{G_0 - A_0}{A_0 + G_1}\right) p_{i,0}^g + \left(\frac{A_0 + A_1}{A_0 + G_1}\right) p_{i,1}^a + \left(\frac{S_A}{A_0 + G_1}\right) \sum_{m=N_x}^{i+1} \left(p_{m,1}^a - p_{m,0}^a\right) \quad (24b)$$

where N_x is the total number of points in the x -direction and with:

$$A_0 = A_1 = \sqrt{\Phi} + \frac{\sigma_0 \Omega_0 \Delta x}{2c_0 \rho_0} \quad (25a)$$

$$G_0 = G_1 = \Omega_0 \quad (25b)$$

$$S_A = \frac{\sigma_0 \Omega_0 \Delta x}{c_0 \rho_0} \quad (25c)$$

Eqs (24) give expressions for the unknown virtual points $p_{i,0}^a$ and $p_{i,1}^g$, and thus allow, used together with the atmospheric and porous ground NPE models, to simulate weakly nonlinear sound propagation over an impedant ground.

3.2. Properties

Limitations: first-order formulations of the constitutive equations have been used to derive the boundary interface condition. This implies that hydrodynamic and Forchheimer's nonlinearities can't be taken into account in the two-way coupling.

Causality: the x -integral present in NPE models (see for example Eq (1)) is calculated from the right to the left of the calculation grid, and the same method is used for coupling (note the sum indexes in Eqs (24)). This ensures that no perturbation is introduced ahead of the point where the wave hits the ground, and thus implies that the interface condition is causal.

Consistency to classical boundary conditions: if one sets $\Phi = +\infty$ we obtain from Eqs (24): $p'_{i,0} = p'_{i,1}$ which is the condition for a totally rigid interface. A transparent interface condition can be obtained by setting $\sigma_0 = 0$, $\Omega_0 = 1$ and $\Phi = 1$ (parameters for an air layer). This leads to: $A_0 = A_1 = 1$ and $G_0 = G_1 = 1$ and thus $p'_{i,0} = p'_{i,0}$ and $p'_{i,1} = p'_{i,1}$. If one sets $\sigma = 0$ and $\Omega_0 = 1$, Eqs (24) become:

$$p'_{i,0} = \frac{\sqrt{\Phi} - 1}{\sqrt{\Phi} + 1} p'_{i,1} + \frac{2}{\sqrt{\Phi} + 1} p'_{i,0} \quad (26)$$

$$p'_{i,1} = \frac{1 - \sqrt{\Phi}}{\sqrt{\Phi} + 1} p'_{i,0} + \frac{2\sqrt{\Phi}}{\sqrt{\Phi} + 1} p'_{i,1} \quad (27)$$

which is the interface condition for two fluid layers with densities ρ_0 and $\sqrt{\Phi}\rho_0$ [2].

Numerical implementation: from a numerical point of view, a common way for solving for diffraction is to use first order finite-differences approximation. This leads to a tridiagonal system of equations that is solved columnwise, from the right to the left of the calculation grid. The boundary interface condition can thus be naturally included in the diffraction solver by imposing values on corresponding points without any additional solver modifications.

4. Numerical examples

In this section some numerical examples of sound propagation over porous ground layers are presented to illustrate the coupling method and evaluate its performances.

4.1. Configuration

In order to verify the correctness of the NPE model developed, results from propagation over impedant ground layers are compared to analytical solutions. The sound speed is constant through the domain ($c_0 = 340 \text{ m.s}^{-1}$), and there is no absorption from air included. Waves decay at a cylindrical rate. The source is positioned at $(x_s, z_s) = (0.0, 1.4) \text{ m}$ and the signal used is a sine pulse with wavelength $\lambda = 0.27 \text{ m}$ ($f = 1259.25 \text{ Hz}$) (the amplitude is low enough for the propagation to be considered linear). A virtual receiver is placed 10 m away from the source and at altitude $z = 1.4 \text{ m}$. The receiver position ensures that we are within the parabolic equation angular validity domain (the angle from source to image–receiver is $\theta \approx 15^\circ$). Spatial steps are equal to $7.5 \cdot 10^{-3} \text{ m}$ in both directions, thus giving a spatial resolution of about 36 points/ λ . The resolution is a bit higher than necessary to ensure sufficient resolution at higher frequencies and near the boundary. The time step is dx/c_0 , so that at each time step the window advances one spatial step. Since semi-implicit schemes are used (Crank-Nicolson method), the CFL condition is satisfied. The NPE window is 3x3 meters (width x height). Three different ground layers of thickness 1 meter are considered. The first ground layer is a perfectly rigid surface ($\Phi \gg 1$). The second and third layers have identical tortuosity ($\Phi = 3$) and porosity ($\Omega_0 = 0.3$), but different flow resistivities ($\sigma_0 = 500 \text{ kPa.s.m}^{-2}$ and $\sigma_0 = 100 \text{ kPa.s.m}^{-2}$).

4.2. Reference solutions

Solutions of the two-dimensional Helmholtz equation are used as references. This solution for the propagation in an homogeneous atmosphere over an impedant ground surface is (for 2-dimensional waves):

$$p_r = i\pi H_0^{(1)}(kR_1) + Qi\pi H_0^{(1)}(kR_2) \quad (28)$$

where p_r is the complex pressure at the receiver, k is the wavenumber, R_1 and R_2 are the source–receiver and image source–receiver distances, respectively, and $H_0^{(1)}$ is the Hankel function of the first kind and order

zero. Q is the cylindrical reflection coefficient and can be calculated with the help of Laplace transforms (see Appendix A1 in [21]). The normalized impedance used to calculate the reflection coefficient is:

$$Z = \sqrt{\frac{\Phi}{\Omega_0^2} + i \frac{\sigma_0}{\rho_0 \Omega_0 \omega}} \quad (29)$$

The real and imaginary parts of the normalized impedances described in section 4.1 are shown in Figure 2.

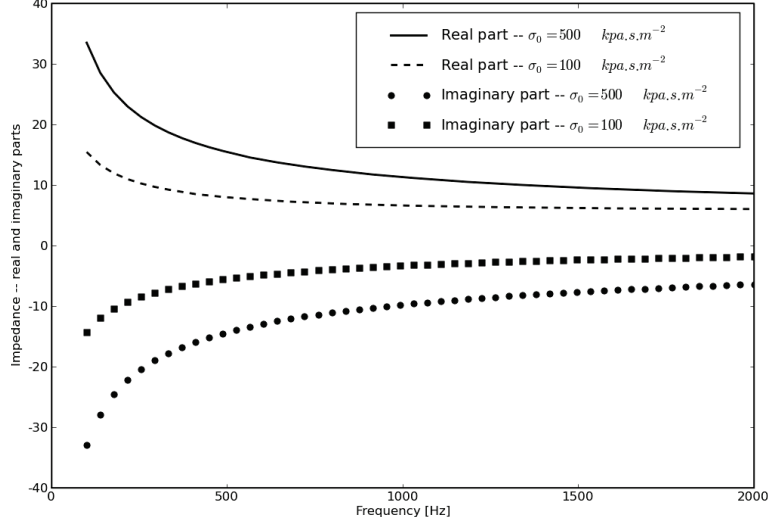


Fig. 2. Real and imaginary parts of the ground layers normalized impedances.

4.3. Results

Figure 3 shows snapshots of the propagation at three different times (from left to right: 3.7, 11.4, 20.2 ms) for the three different ground layers (from top to bottom: rigid, $\sigma_0 = 500 \text{ kpa.s.m}^{-2}$ and $\sigma_0 = 100 \text{ kpa.s.m}^{-2}$). One can see that as the ground is softer, the wave propagate deeper into the layer.

Time signals are recorded at the virtual receiver ($x_r = 10 \text{ m}$, $z_r = 1.4 \text{ m}$); two modifications are done on raw signals: first, in order to obtain a free field reference, time histories are cropped after the direct wave. Original signals are then cleaned for leading spurious oscillations¹. Sound pressure levels (SPLs) relative to free field at the receiver are shown in Figure 4, for both analytical and NPE calculations.

Very good agreement can be observed, independantly of the ground properties: even for the softest layer ($\sigma_0 = 100 \text{ kpa.s.m}^{-2}$) the difference between analytical and NPE calculations is at most about 1 dB. The frequency where negative interference occurs is 1325 Hz, 1273 Hz and 1246 Hz for rigid, hard ($\sigma_0 = 500 \text{ kpa.s.m}^{-2}$) and soft ($\sigma_0 = 100 \text{ kpa.s.m}^{-2}$) layers, respectively. As one can see on Figure 4 the NPE model presented does not only accurately recreate reflected wave amplitude decrease, but does account for this frequency shifting due to the additional delay given during reflection.

5. Including Forchheimer's nonlinearities in the two-way coupling

While flow resistivity dependance on particle velocity (Forchheimer's nonlinearities) are accounted for in the NPE model for porous ground layers (last term in Eq (14)), the two-way coupling between both domains does not contain high-amplitude effects on ground characteristics. This would lead to wrong solutions, since an additional attenuation would be introduced in the ground layer, but the increased rigidity of the interface

¹ This is only necessary for the case where the interface is totally rigid: spurious oscillations, even very weak, prevent obtaining a full negative interference.

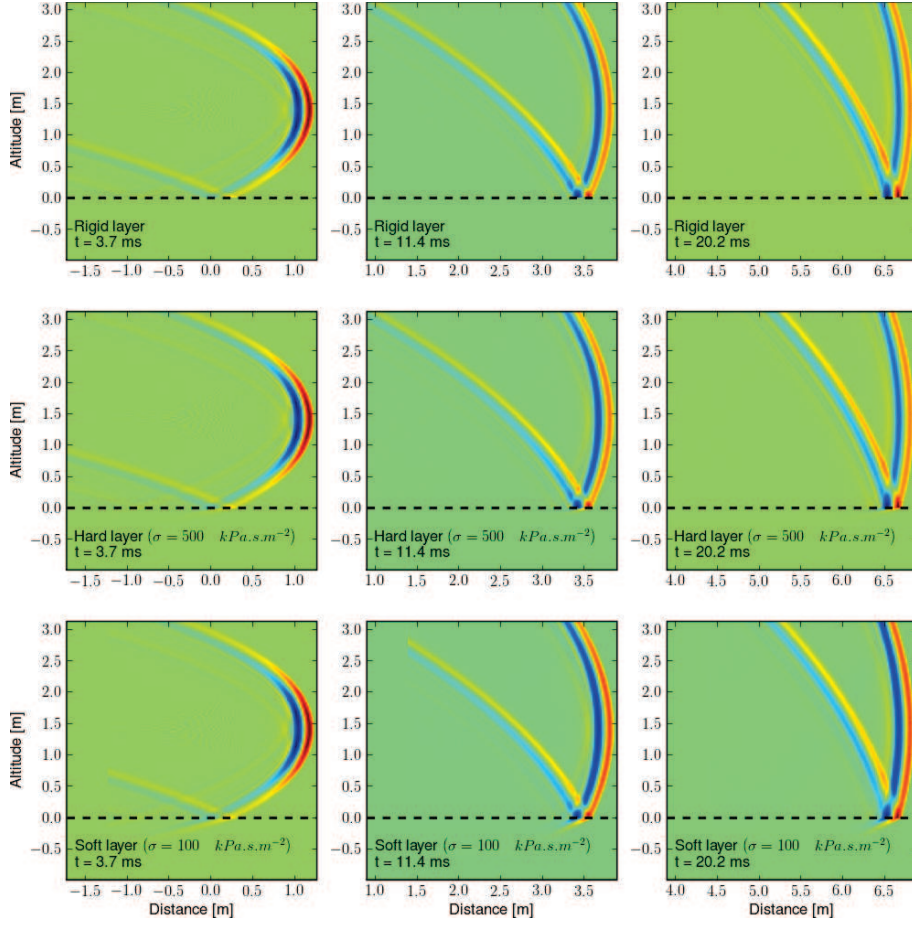


Fig. 3. Snapshots of the propagation at three different times (from left to right: 3.7, 11.4, 20.2 ms) for the three different ground layers (from top to bottom: rigid, $\sigma_0 = 500 \text{ kPa.s.m}^{-2}$ and $\sigma_0 = 100 \text{ kPa.s.m}^{-2}$)

wouldn't be accounted for. A solution is to artificially increase the flow resistivity appearing in the coupling parameters (Eqs (25)) according to:

$$\sigma_0 \longrightarrow \sigma_0 (1 + \xi w^i) \quad (30)$$

where w^i is the vertical particle velocity at the interface. We then use Eq (17) to obtain an approximation of w^i ; we have:

$$w^i = (\rho_0 c_0)^{-1} \int \partial_z p_1^i dx + O(\epsilon^{5/2}) \quad (31)$$

where p_1^i is the first-order approximation of the pressure at the interface. The flow resistivity in the coupling parameters is thus updated according to:

$$\sigma_0 \longrightarrow \sigma_0 \left(1 + \frac{\xi}{\rho_0 c_0} \int \partial_z p_1^i dx \right) \quad (32)$$

At the beginning of each time step, the flow resistivity is thus updated with the help of pressure values at the interface at the previous time step. This method, although approximate, allows to include Forchheimer's nonlinearities in the interfacial condition.

5.1. Numerical example

To illustrate the effects of Forchheimer's nonlinearities a simulation is performed with a ground layer with very low flow resistivity ($\sigma_0 = 10 \text{ kPa.m.s}^{-2}$, $\phi = 3$, $\Omega_0 = 0.3$) and three different Forchheimer's

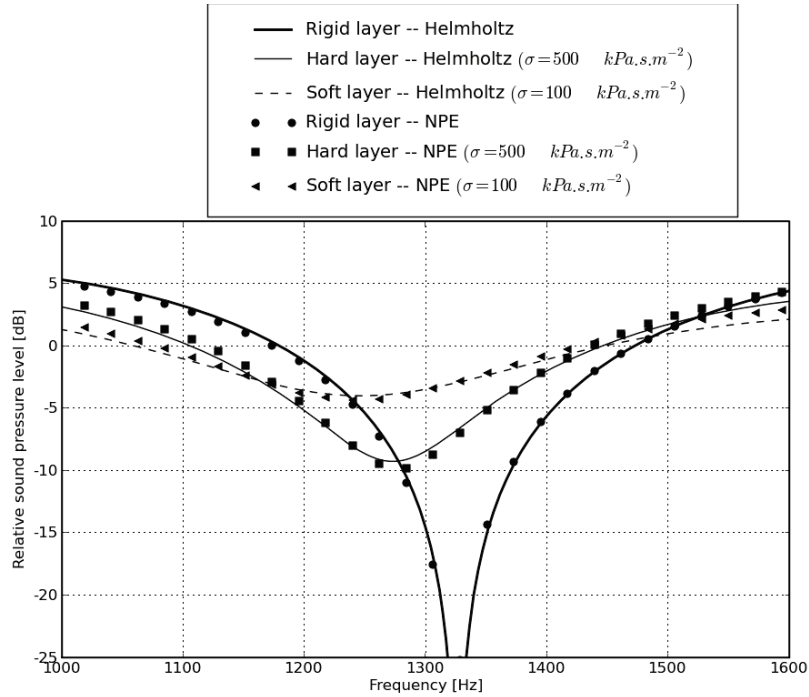


Fig. 4. SPLs relative to free field at the receiver for the three different ground layers, for NPE and analytical solutions. The source and receiver are placed at altitude $z_s = 1.4m$; the receiver is 10 meters away from the source.

nonlinearity parameters: $\xi = 0 \text{ s.m}^{-1}$, $\xi = 2.5 \text{ s.m}^{-1}$ and $\xi = 10 \text{ s.m}^{-1}$. The sound speed is constant through the domain ($c_0 = 340 \text{ m.s}^{-1}$), and there is no absorption from air included. Waves decay at a cylindrical rate. The source is positioned at $(x_s, z_s) = (0, 3) \text{ m}$; the receiver is placed 10 meters away from the source at the same height. Spatial steps are equal to 10^{-2} m in both directions, the NPE window is 4×6 meters (width \times height) and the ground layer is 1 meter thick. The source signal used is a sine pulse with wavelength $\lambda = 0.5 \text{ m}$ ($f = 680 \text{ Hz}$) with peak amplitude $p_0 = 3 \text{ kPa}$. Snapshots of the propagation are shown in Figure 5 for three different times (from left to right: 11.7, 22 and 33.8 ms) for the three different Forchheimer's nonlinearity parameters (from top to bottom: $\xi = 0 \text{ s.m}^{-1}$, $\xi = 2.5 \text{ s.m}^{-1}$ and $\xi = 10 \text{ s.m}^{-1}$). One can see that as the parameter ξ is increased the ground layer becomes more and more rigid and the reflected wave amplitude is higher. Unfortunately no numerical or experimental meaning of validation were available at the time of writing.

6. Conclusion & perspectives

A NPE model based on a nonlinear extension of the Zwicker-Kosten model has been derived; it allows to simulate weakly nonlinear propagation within a porous ground layer. Next, two-way coupling equations have been derived from linearized Euler equations. This interfacial boundary condition couples air and ground NPE models and allows the NPE model to account for the effects of soft ground layers. This method has been shown to give very good agreement with analytical solutions for a wide range of ground properties. It provides a simple but efficient way of taking into account ground impedances. Finally an approximate method to include Forchheimer's nonlinearities in the two-way coupling is presented. In a previous work, the NPE model for porous ground layers and the interfacial condition have been adapted to handle non flat topographies [22]. Two-way coupling equations could also be derived for multilayered ground surfaces without much additional work. With atmospheric refraction and dissipation included, it provides a complete NPE model for weakly nonlinear wave propagation. Propagation of waves from explosions can be simulated

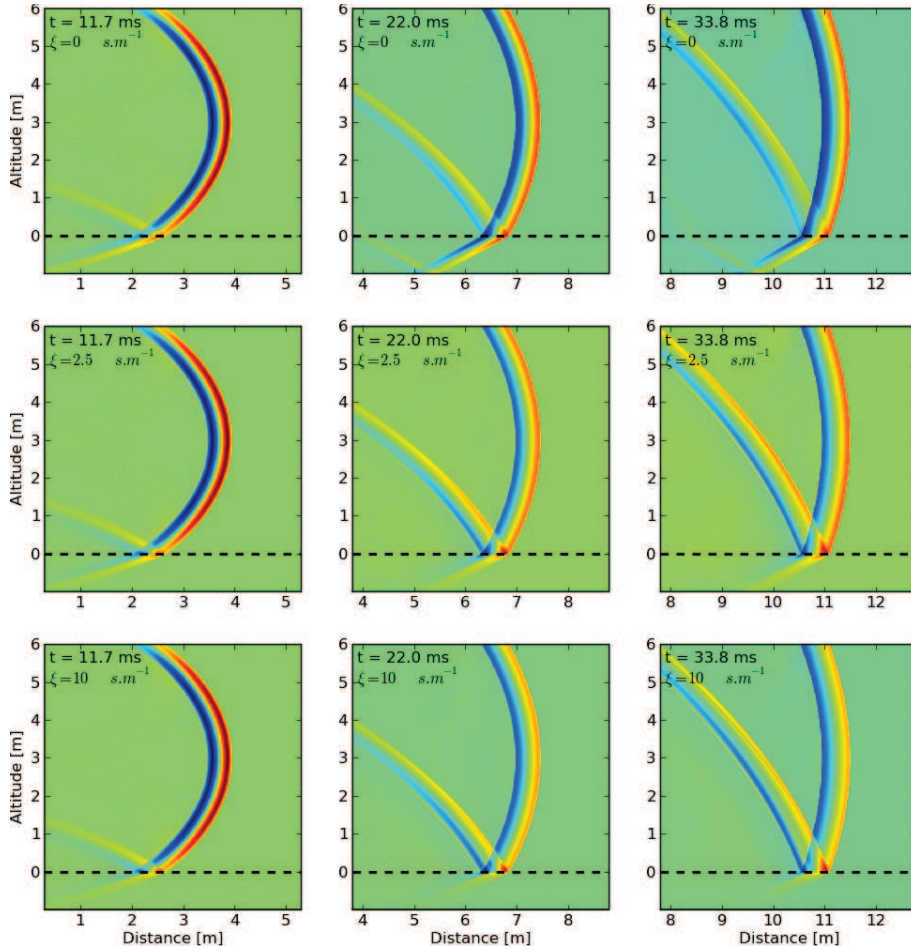


Fig. 5. Snapshots of the propagation at three different times (from left to right: 11.7, 22 and 33.8 ms) for the three different Forchheimer's nonlinearity parameters (from top to bottom: $\xi = 0 \text{ s.m}^{-1}$, $\xi = 2.5 \text{ s.m}^{-1}$ and $\xi = 10 \text{ s.m}^{-1}$).

using a three stages procedure: first, a method based on Euler equations is used in the near field, where the propagation is highly nonlinear. Next, NPE models can propagate weakly nonlinear waves over moderate distances and finally, when the wave amplitude is low enough, (linear) frequency-domain method like the PE can be used. This hybrid method allows to propagate waves from explosions over distances up to several kilometres [4].

References

- [1] B. E. McDonald, W. A. Kuperman, Time domain formulation for pulse propagation including nonlinear behaviour at a caustic, *J. Acoust. Soc. of Am.* 81 (1987) 1406–1417.
- [2] J. J. Ambrosiano, D. R. Plante, B. E. McDonald, W. A. Kuperman, Nonlinear propagation in an ocean acoustic waveguide, *J. Acoust. Soc. of Am.* 87 (1990) 1473–1481.
- [3] K. Castor, P. Gerstoft, P. Roux, B. McDonald, W. Kuperman, Long-range propagation of finite-amplitude acoustic waves in an ocean waveguide, *J. Acoust. Soc. America* 116 (4) (2004) 2004–2010.
- [4] F. van der Eerden, E. Védý, Propagation of shock waves from source to receiver, *Noise Control Eng. J.* 53 (2005) 87–93.
- [5] K. Attenborough, P. Schomer, E. Védý, F. van der Eerden, Overview of the theoretical development and experimental validation of blast sound-absorbing surfaces, *Noise Control Eng. J.* 53 (3) (2005) 70–80.
- [6] K. Attenborough, A. Cummings, P. Dutta, P. Schomer, E. Salomons, E. Standley, O. Umnova, F. van den Berg, F. van der Eerden, P. van der Weele, E. Védý, Blast sound absorbing surfaces, Tech. rep., ERDC/CRREL (September 2004).

- [7] T. Leissing, Nonlinear outdoor sound propagation – A numerical implementation and study using the nonlinear progressive wave equation, Master’s thesis, Chalmers University of Technology (2007).
URL <http://documents.vsect.chalmers.se/CPL/exjobb2007/ex2007-013.Pdf>
- [8] B. E. McDonald, P. Caine, M. West, A tutorial on the nonlinear progressive wave equation (NPE) - Part 1, *Applied Acoustics* 43 (1994) 159–167.
- [9] P. Caine, M. West, A tutorial on the nonlinear progressive wave equation (NPE) - Part 2. derivation of the three dimensional cartesian version without use of perturbation expansions, *Applied Acoustics* 45 (1995) 155–165.
- [10] B. E. McDonald, Weak shock interaction with a free-slip interface at low grazing angles, *J. Acoust. Soc. America* 91 (2) (1992) 718–733.
- [11] G. P. Too, J. H. Ginsberg, Cylindrical and spherical coordinate versions of the NPE for transient and steady-state sound beams, *J. Vib. Acoust.* 114 (1992) 420–424.
- [12] G. P. J. Too, S. T. Lee, Thermoviscous effects on transient and steady-state sound beams using nonlinear progressive wave equation models, *J. Acoust. Soc. of Am.* 97 (1995) 867–874.
- [13] B. E. McDonald, High-angle formulation for the nonlinear progressive wave equation model, *Wave Motion* 31 (2000) 165–171.
- [14] P. Blanc-Benon, B. Lipkens, L. Dallois, M. F. Hamilton, D. T. Blackstock, Propagation of finite-amplitude sound through turbulence: Modeling with geometrical acoustics and the parabolic approximation, *J. Acoust. Soc. of Am.* 111 (2002) 487–498.
- [15] C. Zwikker, C. W. Kosten, *Sound absorbing materials*, Elsevier, 1949.
- [16] A. Krylov, S. Sorek, A. Levy, G. Ben-Dor, Simple waves in saturated porous media (I. The isothermal case), *JSME international journal* 39 (1996) 294–298.
- [17] E. Védý, Simulations of flows in porous media with a flux corrected transport algorithm, *Noise Control Eng. J.* 50 (2002) 211–217.
- [18] O. Umnova, K. Attenborough, A. Cummings, High amplitude pulse propagation and reflection from a rigid porous layer, *Noise Control Eng. J.* 50 (2002) 204–210.
- [19] For example, Eq (31) in [8], or Eq (39) in [9].
- [20] Eq (19) is given as Eq (10) in [21].
- [21] E. M. Salomons, R. Blumrich, D. Heimann, Eulerian time-domain model for sound propagation over a finite impedance ground surface. Comparison with frequency-domain models, *Acta Acustica United With Acustica* 88 (2002) 483–492.
- [22] T. Leissing, P. Jean, J. Defrance, C. Soize, Nonlinear parabolic equation model for finite-amplitude sound propagation in an inhomogeneous medium over a nonflat, finite-impedance ground surface, in: *Proceedings of EuroNoise 08, Paris, 2008*.